Provided for non-commercial research and education use.
Not for reproduction, distribution or commercial use.

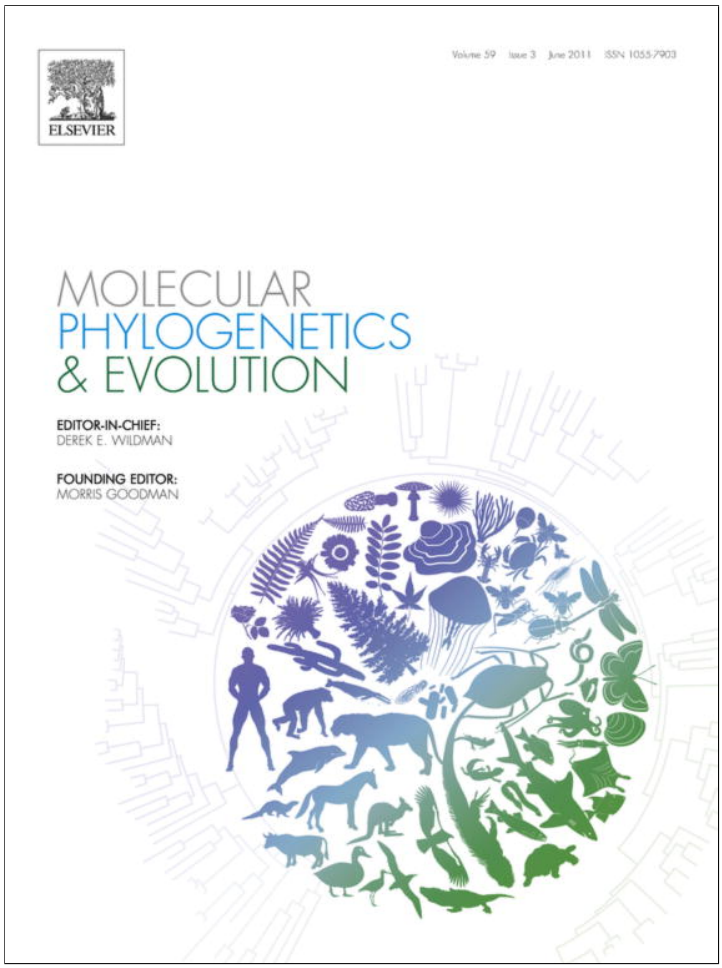

This article appeared in a journal published by Elsevier. The attached copy is furnished to the author for internal non-commercial research and education use, including for instruction at the authors institution and sharing with colleagues.

Other uses, including reproduction and distribution, or selling or licensing copies, or posting to personal, institutional or third party websites are prohibited.

In most cases authors are permitted to post their version of the article (e.g. in Word or Tex form) to their personal website or institutional repository. Authors requiring further information regarding Elsevier's archiving and manuscript policies are encouraged to visit:

http://www.elsevier.com/copyright

Author's personal copy

Molecular Phylogenetics and Evolution 59 (2011) 603–614

Contents lists available at ScienceDirect

Molecular Phylogenetics and Evolution

journal homepage: www.elsevier.com/locate/ympev

A phylogenetic analysis of the boreal lichen *Mycoblastus sanguinarius* (Mycoblastaceae, lichenized Ascomycota) reveals cryptic clades correlated with fatty acid profiles

Toby Spribille *, Barbara Klug, Helmut Mayrhofer

Institute of Plant Sciences, University of Graz, Holteigasse 6, A-8010 Graz, Austria

ARTICLE INFO

Article history:
Received 16 August 2010
Revised 24 December 2010
Accepted 17 March 2011
Available online 30 March 2011

Keywords:
Aliphatic compound
Ascomycete
Chemotaxonomy
Cryptic species
Internal transcribed spacer region
Lichen chemistry
Replication licensing factor Mcm7 gene
Translation elongation factor 1-α gene

ABSTRACT

Lichens are a prominent feature of northern conifer forests and a large number of species are thought to be circumboreal. Whether or not circumboreal lichen species really constitute monophyletic groups has seldom been tested. We investigated molecular phylogenetic patterns in the mycobiont of *Mycoblastus sanguinarius*, a well known epiphytic lichen species of the boreal forest, based on material collected from across the high latitude northern hemisphere. A three-locus dataset of internal transcribed spacer rDNA, translation elongation factor 1-α and replication licensing factor Mcm7 DNA sequences revealed that material treated until now as belonging to *M. sanguinarius* does indeed form a monophyletic group within the genus and is distinct from a strongly supported *Mycoblastus affinis*. The *M. sanguinarius* complex appears closely related to the rare *Mycoblastus glabrescens*, which is currently known only from the Pacific Northwest and was rediscovered during the present study. However, within *M. sanguinarius* s.lat. in the northern hemisphere, two deeply divergent and morphologically coherent species can be recovered, one of which matches the southern hemisphere species *Mycoblastus sanguinarioides* and turns out to be widespread in North America and Asia, and one of which corresponds to *M. sanguinarius* s.str. Both *M. sanguinarius* and *M. sanguinarioides* exhibit additional low-level genetic differentiation into geographically structured clades, the most prominent of which are distributed in East Asia/eastern North America and western North America/Europe, respectively. Individuals from these lowest-level clades are morphologically indistinguishable but chemical analyses by thin layer chromatography revealed that each clade possesses its own fatty acid profile, suggesting that chemical differentiation precedes morphological differentiation and may be a precursor to speciation.

© 2011 Elsevier Inc. All rights reserved.

1. Introduction

Many lichen species occurring at high latitudes have a circumboreal distribution, i.e., they occur around the northern hemisphere in the zone of boreal coniferous forests. There is no single worldwide survey of precisely how many species share this distribution, but rough estimates suggest that it may be as much as 60–70% of the macrolichen floras in regions such as northern Europe or eastern North America, and over 1000 species in total (Ahti, 1977; Printzen, 2008). Much of what we assume today about species having circumboreal distributions dates from an era when European-based taxonomic concepts were still applied through keys to two of the world's most biodiverse high latitude regions, northwest North America and the Russian Far East. It is thus an open question how many circumboreal species, upon detailed phylogenetic study, will actually be found to be monophyletic.

Results of the few phylogenetic studies in widespread lichen species up to now have been mixed when it comes to reporting hidden taxa. Molecular phylogenetic studies at lower, temperate latitudes have revealed extensive cryptic speciation or clade differentiation in lichenized fungi (Kroken and Taylor, 2001; Crespo et al., 2002; Buschbom and Mueller, 2006; Argüello et al., 2007; Divakar et al., 2010). Such 'cryptic species' are in some cases confirmation of subtle morphological patterns already detected and named by taxonomists and in other cases they are lineages that have genuinely been missed in all taxonomic studies (Crespo and Pérez-Ortega, 2009). At the same time, Geml et al. (2010) have shown that in at least two widespread arctic–alpine lichen fungi (*Flavocetraria cucullata* and *Flavocetraria nivalis*) molecular phylogenies support current morphology-based species delimitations, suggesting not all currently accepted species are necessarily repositories of hidden diversity.

No circumboreal lichen species has yet been studied using a molecular phylogenetic approach across its entire range, but doing so may provide insights into the phylogenetic diversity potentially

* Corresponding author.
E-mail address: toby.spribille@uni-graz.at (T. Spribille).

1055-7903/$ - see front matter © 2011 Elsevier Inc. All rights reserved.
doi:10.1016/j.ympev.2011.03.021

Author's personal copy

concealed within such species. After screening numerous taxa with this distribution for their suitability for such a study, we chose *Mycoblastus sanguinarius* (L.) Norman, a common and easily recognized member of the circumboreal element reported from across the northern hemisphere. *M. sanguinarius* is one of the original 80 lichen taxa recognized by Linnaeus (1753) in the first edition of his Species Plantarum (as *Lichen sanguinarius*), and is a well-known lichen species of the boreal forest, where it typically grows on conifer bark and wood. It is easily recognized on account of a deep red pigment (mysaquinone, also known as rhodocladonic acid) in the tissue below the apothecium, often visible even in the field after being exposed by snail grazing, giving rise to the common name 'bloody heart lichen'. In addition to Scandinavia, it is also known from Greenland, Scotland, the central European mountain ranges, across Russia to the Sea of Okhotsk and Japan, and across the northern half of North America (Brodo et al., 2001; Andreev et al., 2008). Scattered disjunct occurrences are known from high mountains at lower latitudes. Reports of the species from the southern hemisphere have in part been revised to belong to another putatively closely related species, *Mycoblastus sanguinarioides* (Kantvilas, 2009).

Interest in the variation within *M. sanguinarius* began in the mid-19th century, and much of it revolved around forms that lacked the red pigment below the apothecia. An arctic–alpine form on moss was recognized already in 1831 as var. *alpinus*, and was later raised to species rank (*Mycoblastus alpinus* [Fr.] Hellb.). In 1850, the Swiss botanist Schaerer was the first to recognize the unpigmented form as a separate species that later came to be called *Mycoblastus affinis* (Schaer.) T. Schauer (Schauer, 1964; syn. *Mycoblastus melinus* [Kremp.] Hellb.). However, in the absence of chemical and molecular insights, speculation continued that *M. affinis* and even *M. alpinus* were merely forms of *M. sanguinarius* (Anders, 1928). Some Fennoscandian lichenologists took a more splitting view and not only recognized *M. affinis* and *M. alpinus*, but also began parsing *M. sanguinarius* into several infraspecific varieties and forms based on degree of pigmentation, size of apothecia, and presence or absence of a thalline tissue rim around the apothecia (Nylander, 1890; Wainio, 1909). One other species with red pigment below the apothecia, *Mycoblastus japonicus* Müll.Arg., was described from Japan and continues to be known only from eastern Asia. Another widespread northern hemisphere taxon, *Mycoblastus fucatus* (Stirt.) Zahlbr., differs from other species of *Mycoblastus* in its anomalous ascocarp characters and its assignment to *Mycoblastus* is uncertain. The introduction of microchemical and chromatographic methods in the 20th century revolutionized lichen taxonomy and also came to bear on *Mycoblastus*. Tønsberg (1992) and Huneck and Schmidt (1995) were the first to discover the chemical distinctness of *M. affinis* and *M. japonicus*, respectively, from *M. sanguinarius* in their secondary compounds. Tønsberg was also the first to investigate fatty acids in *Mycoblastus*, followed later by Kantvilas (2009), although in both cases a relatively small number of samples were investigated. Kantvilas (2009) also resurrected an obscure Pacific Northwest taxon, *Mycoblastus glabrescens* (Nyl.) Zahlbr., known only from a single specimen and likewise distinguished by a fatty acid. Otherwise no comprehensive survey has been undertaken of *Mycoblastus* chemistry to date.

Notwithstanding the untested nature of the species delimitations of *M. sanguinarius* relative to *M. affinis* and *M. japonicus*, it appears relatively few taxa are involved compared to many other boreal species complexes. Even so, we were well aware that morphological coherence in a taxon such as *M. sanguinarius* does not necessarily predict monophyly. We were prepared to face one of three scenarios: (1) *M. sanguinarius* could indeed include unpigmented forms and chemical variability and should be broadly defined; (2) *M. sanguinarius* as currently defined is supported by molecular evidence; or (3) *M. sanguinarius* as currently defined is too broad and supports possibly overlooked but genetically well marked cryptic taxa. We accordingly cast a broad net during field sampling and collected numerous individual thalli regardless of whether apothecia had red pigment and to which taxon they ostensibly belonged. Our overarching aim is to identify a widespread monophyletic group to serve as model species for more detailed studies into circumboreal diversification and gene flow. To this end, the objectives of the present study are threefold: (1) we will provide a phylogenetic framework for the relationship of *M. sanguinarius* to other taxa (*M. affinis*, *M. alpinus*, *M. fucatus*, *M. glabrescens*, *M. japonicus* and *M. sanguinarioides*) for which various degrees of relatedness have been proposed; (2) we will identify phylogenetic signal within *M. sanguinarius* s.str. using samples from across its range without any a priori hypotheses about the significance of morphological characters, with the aim of identifying recognizable, operational taxonomic units for future population genetic analysis; and (3) we will examine the resulting clades for patterns that correlate to morphology and secondary chemistry.

2. Materials and methods

2.1. DNA extraction and sequencing

Specimens of *M. sanguinarius* s.lat. and related taxa were collected throughout the high latitude northern hemisphere during 2008–2009 (Table 1). Specimens were air dried and stored at room temperature until preparation; all vouchers are retained in the herbarium GZU unless otherwise noted and are annotated with the isolate numbers used in Table 1. Material for DNA extraction was taken from apothecia if present, otherwise from parasite-free thallus fragments inspected in water droplets on a microscope slide under 20× magnification. Prepared material was transferred into reaction tubes, dried and pulverized using a TissueLyserII (Retsch). DNA was extracted using the DNeasy Plant Mini Kit (Qiagen) extraction kit using the manufacturer's instructions.

Dilutions (mostly 5×10^{-2}) of the genomic DNA extractions were used to obtain PCR products for the three markers. We screened a set of about ten molecular markers for a balance of reliability of obtaining PCR products and sufficient levels of sequence variability, finally selecting three loci for this study: two protein-coding genes, namely translation elongation factor 1-α (EF1-α) and the DNA replication licensing factor mini-chromosome maintenance complex 7 (Mcm7), and the nuclear ribosomal internal transcribed spacer region (ITS) (Table 2). 25 μl PCR reactions were performed with Illustra Ready-To-Go RT-PCR Beads (GE Healthcare) in a thermocycler (AlphaMetrix) using the following programs: EF1-α: initial denaturation 2 min at 95 °C, touchdown 9 cycles: 95 °C 1 min, 66–57 °C 30 s, 72 °C 1 min, followed by 36 cycles 95 °C 30 s, 56 °C 30 s, 72 °C 1 min and a final extension of 10 min at 72 °C; ITS: initial denaturation 95 °C 3 min, 35 cycles 95 °C 1 min, 52 °C 1 min, 72 °C 1.5 min, final extension 72 °C 7 min; Mcm7: initial denaturation 10 min at 95 °C, touchdown 6 cycles: 95 °C 45 s, 60–55 °C 50 s, 72 °C 1 min, followed by 38 cycles: 95 °C 45 s, 56 °C 50 s, 72 °C 1 min and a final extension of 5 min at 72 °C. 2 μl aliquots of PCR products were viewed on 1% agarose gels stained with GelRed™ (Biotium, VWR) and subsequently purified with NucleoSpin Extract II Kit (Macherey–Nagel). PCR product sequencing was outsourced to Macrogen, Inc. (Seoul, South Korea). Obtained sequence fragments were obtained electronically from Macrogen, subjected to a BLAST search to control for correct taxonomic neighborhood and checked for electropherogram ambiguities in BioEdit (Hall, 1999). All DNA sequences were

Table 1
DNA sequence vouchers used in this study and their GenBank accession numbers. All specimens are deposited in GZU unless otherwise indicated.

Isolate Code	Locality	Collector and number	Latitude	Longitude	GenBank Accession Number		
					EF1-α	ITS	MCM7
Mycoblastus affinis s.lat. (including *M. alpinus*)							
AFF90	Philip Lake, Wells Gray Prov. Park, British Columbia, Canada	Goward & Wright s.n.	51°52′15.13″N	119°55′52.48″W	JF744895	JF744969	JF744809
AFF121	Russian River, Kenai Peninsula, Alaska, U.S.A.	Spribille 27371	60°28.970′N	149°56.631′W	JF744896	–	JF744812
AFF379	Laughing Water Creek, Lincoln Co., Montana, U.S.A.	Spribille 30126	48°44.711′N	114°51.140′W	JF744898	JF744980	JF744795
AFF420	Steinerkogel, near Oberzeiring, Steiermark, Austria	Spribille 30220	47°16.245′N	014°25.243′E	JF744899	JF744978	JF744797
AFF464	Dreisesselberg, Bavaria, Germany	Spribille 32115	48°47′27.82″N	13°47′29.58″E	JF744900	JF744979	JF744800
AFF465	Hörsterkogel, Steiermark, Austria	Spribille 32102	47°35′24.70″N	15°19′37.76″E	JF744902	JF744977	JF744801
AFF466	LaBiche River, Yukon Territory, Canada	Spribille 28541	60°09.037′N	124°05.385′W	JF744903	–	JF744802
AFF766	Cape Breton Highlands, Nova Scotia, Canada	Spribille & Wagner, 05.10.09, s.n.	46°49.389′N	60°39.680′W	JF744897	–	JF744813
ALP468	White Pass, Skagway Borough, Alaska, U.S.A.	Spribille 26781 (KLGO)	59°37.033′N	135°09.800′W	JF744904	–	JF744803
ALP537	Lac à Jack, Réserve Faunique des Laurentides, Québec, Canada	Spribille & Wagner, 28.09.09, s.n.	47°36.302′N	70°59.307′W	JF744901	JF744976	JF744805
Mycoblastus fucatus							
FUC600	Mt Greylock, Berkshire Co., Massachusetts, U.S.A.	Spribille 32161	42°38.231′N	73°10.208′W	–	JF744968	JF744818
Mycoblastus glabrescens							
GLA92	Elk Pass, Skamania Co., Washington, U.S.A.	Spribille 29848	46°17.250′N	121°58.469′W	JF744894	JF744967	JF744810
GLA352	Hobo Cedar Grove Botanical Area, Shoshone Co., Idaho, U.S.A.	Spribille 30024	47°05.167′N	116°06.793′W	JF744893	JF744985	JF744816
GLA367	Tombstone Pass, Linn Co., Oregon, U.S.A.	Spribille 29899	44°23.706′N	122°08.493′W	JF744892	JF744984	JF744815
Mycoblastus japonicus							
JAP802	Sorak-san National Park, Gangwon Province, South Korea	Thor 20551 (UPS)	3806.45-28′N	12826.00-25.10′E	–	JF744983	–
Mycoblastus sanguinarioides							
SAID85	Skeena River area, near Kispiox, British Columbia, Canada	Spribille 29811-B	55°32.933′N	127°43.625′W	JF744883	JF744965	JF744807
SAID86	Bijoux Falls, British Columbia, Canada	Spribille 26159	55°18.499′N	122°40.277′W	JF744881	–	JF744808
SAID117	Russian River, Kenai Peninsula, Alaska, U.S.A.	Spribille 27367	60°28.970′N	149°56.631′W	JF744890	JF744970	JF744811
SAID250	Chilkoot Trail, Klondike Gold Rush National Historical Park, Alaska, U.S.A.	Spribille 27038-A	59°34.652′N	135°19.766′W	JF744884	JF744971	JF744794
SAID389	Divide between Chistiy and Khanda River watersheds, W of De Kastri, Khabarovskiy Krai, Russia	Spribille 31111	51°23.260′N	140°21.758′E	JF744885	JF744975	JF744796
SAID422	Pravaya Bureya River, Bureinskiy Zapovednik, Khabarovskiy Krai, Russia	Spribille 31866	52°09.604′N	134°19.697′E	–	–	JF744798
SAID460	10 km W of DeKastri, Khabarovskiy Krai, Russia	Spribille 30655	51°26.743′N	140°38.357′E	JF744886	JF744974	JF744799
SAID525	Khomi Mountains, just S of mountain 'Shaman', Khabarovskiy Krai, Russia	Spribille 30614	51°24.172′N	139°59.485′E	–	JF744964	JF744804
SAID539	Hwy 7 SW of Sherbrooke, Nova Scotia, Canada	Spribille & Wagner, 06.10.09, s.n.	45°06.499′N	62°00.453′W	JF744887	JF744982	–
SAID542	Advocate Harbour, Nova Scotia, Canada	Spribille & Wagner, 08.10.09, s.n.	45°20.248′N	64°44.550′W	JF744888	JF744981	JF744806
SAID581	Track to Lake Nicholls, Tasmania, Australia	Kantvilas 348/08	42°40′S	146°39′E	–	JF744973	JF744820
SAID582	Foot of Adams Peak, Tasmania, Australia	Kantvilas 1/09	41°44′S	146°41′E	JF744889	JF744972	JF744819
SAID633	St. Croix River, Charlotte Co., New Brunswick, Canada	Clayden 16162 (NBM)	45.32°N	67.43′W	JF744882	JF744966	JF744817
SAID760	Jefferson Notch, Coos Co., New Hampshire, U.S.A.	Spribille & Wagner, 23.09.09, s.n.	44°17.793′N	71°21.284′W	JF744891	JF744963	JF744814
Mycoblastus sanguinarius							
SANG73	Hobo Cedar Grove Botanical Area, Shoshone Co., Idaho, U.S.A.	Spribille 30026-A	47°05.167′N	116°06.793′W	JF744822	JF744909	JF744741
SANG77	Laughing Water Creek, Lincoln Co., Montana, U.S.A.	Spribille 30127-A	48°44.711′N	114°51.140′W	JF744823	JF744910	JF744742
SANG79	Dawson Falls, Wells Gray Prov. Park, British Columbia, Canada	Spribille 26152	51°57.824′N	120°07.695′W	JF744824	JF744911	JF744743
SANG81	Cowlitz River, Skamania Co., Washington, U.S.A.	Spribille 29839-A	46°39.507′N	121°36.131′W	JF744825	JF744912	JF744744
SANG94	Chena River, E of Fairbanks, Alaska, U.S.A.	Spribille 27614	64°53.665′N	146°41.428′W	JF744826	–	JF744745
SANG100	Retallack, British Columbia, Canada	Spribille 30134-A	50°02.527′N	117°09.027′W	JF744879	JF744913	JF744746
SANG120	Russian River, Kenai Peninsula, Alaska, U.S.A.	Spribille 27370	60°28.970′N	149°56.631′W	JF744827	JF744914	JF744747
SANG123	Russian River, Kenai Peninsula, Alaska, U.S.A.	Spribille 27373	60°28.970′N	149°56.631′W	JF744828	JF744915	JF744748
SANG124	Hartelsgraben, Nationalpark Gesäuse, Steiermark, Austria	Spribille 30207-A	47°35.138′N	014°42.341′E	JF744872	–	JF744749
SANG128	Hartelsgraben, Nationalpark Gesäuse, Steiermark, Austria	Spribille 30201-C	47°35.138′N	014°42.341′E	JF744829	JF744916	JF744750
SANG129	Hartelsgraben, Nationalpark Gesäuse, Steiermark, Austria	Spribille 30201-D	47°35.138′N	014°42.341′E	JF744830	JF744917	JF744751
SANG130	Hartelsgraben, Nationalpark Gesäuse, Steiermark, Austria	Spribille 30207-B	47°35.138′N	014°42.341′E	JF744831	JF744918	JF744752
SANG131	Hartelsgraben, Nationalpark Gesäuse, Steiermark, Austria	Spribille 30201-E	47°35.138′N	014°42.341′E	JF744832	JF744919	JF744753
SANG135	Mt. Blaxas, Forsa Parish, Hälsingland, Sweden	Wedin 8295	61°38′29.6″N	16°46′40.8″E	JF744833	JF744920	JF744754
SANG136	Mt. Blaxas, Forsa Parish, Hälsingland, Sweden	Wedin 8297	61°38′29.6″N	16°46′40.8″E	JF744834	JF744921	JF744755
SANG138	Mt. Blaxas, Forsa Parish, Hälsingland, Sweden	Wedin 8290	61°38′29.6″N	16°46′40.8″E	–	JF744922	JF744756
SANG141	Mt. Blaxas, Forsa Parish, Hälsingland, Sweden	Wedin 8288	61°38′29.6″N	16°46′40.8″E	JF744835	JF744923	JF744757
SANG142	Mt. Blaxas, Forsa Parish, Hälsingland, Sweden	Wedin 8299	61°38′29.6″N	16°46′40.8″E	JF744836	JF744924	JF744758
SANG152	Reserva Integral de Muniellos, Asturias, Spain	Spribille 30264-D	43°01.922′N	6°41.654′W	JF744837	JF744925	–

(*continued on next page*)

Author's personal copy

Author's personal copy

Table 1 (*continued*)

Isolate Code	Locality	Collector and number	Latitude	Longitude	GenBank Accession Number		
					EF1-α	ITS	MCM7
SANG156	Reserva Integral de Muniellos, Asturias, Spain	Spribille 30264-F	43°01.922′N	6°41.654′W	JF744838	JF744926	JF744759
SANG159	Reserva Integral de Muniellos, Asturias, Spain	Spribille 30264-I	43°01.922′N	6°41.654′W	JF744839	JF744927	JF744760
SANG161	Reserva Integral de Muniellos, Asturias, Spain	Spribille 30264-K	43°01.922′N	6°41.654′W	JF744840	JF744928	JF744761
SANG165	Åsane, Hordaland, Norway	Spribille 30237-E	60°27.373′N	005°18.328′E	JF744844	JF744929	–
SANG166	Åsane, Hordaland, Norway	Spribille 30237-F	60°27.373′N	005°18.328′E	JF744841	JF744930	JF744762
SANG167	Åsane, Hordaland, Norway	Spribille 30237-K	60°27.373′N	005°18.328′E	JF744842	JF744931	JF744763
SANG169	Åsane, Hordaland, Norway	Spribille 30237-H	60°27.373′N	005°18.328′E	JF744880	JF744932	JF744764
SANG170	Åsane, Hordaland, Norway	Spribille 30237-I	60°27.373′N	005°18.328′E	JF744843	JF744905	JF744765
SANG175	Tavelsjö Parish, Västerbotten, Sweden	Wedin 8336	64°02′36.4′N	20°18′07.8‘‘E	JF744845	JF744933	–
SANG177	Tavelsjö Parish, Västerbotten, Sweden	Wedin 8338	64°02′36.4′N	20°18′07.8‘‘E	JF744846	JF744934	JF744766
SANG180	Tavelsjö Parish, Västerbotten, Sweden	Wedin 8342	64°02′36.4′N	20°18′07.8‘‘E	JF744847	JF744935	JF744767
SANG181	Tavelsjö Parish, Västerbotten, Sweden	Wedin 8343	64°02′36.4′N	20°18′07.8‘‘E	JF744848	JF744936	JF744768
SANG185	Western Beskidy Mtns., Gorce Mtns., Poland	Czarnota 121008/8	49°33.150′N	20°07.183′E	JF744849	JF744937	JF744769
SANG188	Western Beskidy Mtns., Gorce Mtns., Poland	Czarnota 121008/4	49°33.150′N	20°07.183′E	JF744850	JF744938	JF744770
SANG189	Western Beskidy Mtns., Gorce Mtns., Poland	Czarnota 121008/9	49°33.150′N	20°07.183′E	JF744851	JF744939	JF744771
SANG190	Western Beskidy Mtns., Gorce Mtns., Poland	Czarnota 121008/10	49°33.150′N	20°07.183′E	JF744852	JF744940	JF744772
SANG192	Western Beskidy Mtns., Gorce Mtns., Poland	Czarnota 121008/2	49°33.150′N	20°07.183′E	JF744853	JF744941	JF744773
SANG194	Steinkjer, W of Lauvåsen, Nord-Trøndelag, Norway	Holien 11926-A	64°03′10‘‘N	11° 32′18‘‘E	JF744854	JF744942	JF744774
SANG199	Steinkjer, W of Lauvåsen, Nord-Trøndelag, Norway	Holien 11926-B	64°03′10‘‘N	11° 32′18‘‘E	JF744855	JF744943	JF744775
SANG228	Tokositna River, Denali National Park, Alaska, U.S.A.	Spribille 27824	62°39.148′N	150°47.410′W	JF744857	–	JF744776
SANG236	Along Hwy. 26 SE of Mt. Hood, Wasco Co., Oregon, U.S.A.	Spribille 29881-C	45°09.666′N	121°38.636′W	JF744858	JF744944	JF744777
SANG237	Along Hwy. 26 SE of Mt. Hood, Wasco Co., Oregon, U.S.A.	Spribille 29881-D	45°09.666′N	121°38.636′W	JF744859	JF744906	–
SANG242	Along Hwy. 26 SE of Mt. Hood, Wasco Co., Oregon, U.S.A.	Spribille 29881-I	45°09.666′N	121°38.636′W	JF744860	JF744945	JF744778
SANG245	Chilkoot Trail, Klondike Gold Rush National Historical Park, Alaska, U.S.A.	Spribille 27038-B	59°34.652′N	135°19.766′W	JF744878	JF744946	–
SANG267	Dawson Falls, Wells Gray Prov. Park, British Columbia, Canada	Spribille 26151	51°57.824′N	120°07.695′W	JF744861	JF744947	JF744779
SANG329	West Twin Provincial Park, British Columbia, Canada	Spribille 29832-A	53°26.379′N	120°30.390′W	JF744862	JF744948	JF744780
SANG398	Between Umal'ta and Nimakan Rivers, Khabarovskiy Krai, Russia	Spribille 31603	51°47.546′N	133°21.122′E	JF744863	JF744907	–
SANG410	Stream 'Lesosechnaya', Etkil'-Yankanskiy Mountains, Khabarovskiy Krai, Russia	Spribille 31330	51°47.285′N	135°39.166′E	JF744864	JF744949	JF744781
SANG436	Sredniy Khrebet, between streams Studeniy and Zvuchnaya, near Lazarev, Khabarovskiy Krai, Russia	Spribille 30949	52°13.451′N	141°00.428′E	–	JF744950	JF744782
SANG446	Mountain 'Arbat', De Kastri, Khabarovskiy Krai, Russia	Spribille 30743	51°25.171′N	140°44.404′E	JF744865	–	JF744783
SANG447	Mountain 'Arbat', De Kastri, Khabarovskiy Krai, Russia	Spribille 30744	51°25.171′N	140°44.404′E	–	JF744951	JF744784
SANG481	Arvidsjaur Parish, Pite Lappmark, Sweden	Muggia s.n.	65.983340°N	19.345340°E	–	JF744952	JF744785
SANG493	Mt. O-akan, Kushiro Subprefecture, Hokkaido, Japan	Ohmura 6746	43°26′41.8‘‘N	144°09′02.9‘‘E	JF744866	JF744953	JF744786
SANG498	Mt. O-akan, Kushiro Subprefecture, Hokkaido, Japan	Ohmura 6750	43°26′41.8‘‘N	144°09′02.9‘‘E	–	JF744954	–
SANG503	Mt. O-akan, Kushiro Subprefecture, Hokkaido, Japan	Ohmura 6738	43°26′41.8‘‘N	144°09′02.9‘‘E	JF744874	JF744955	–
SANG543	Along Route 138 N of Les Escoumins, Québec, Canada	Spribille & Clayden s.n.	48°25.481′N	69°19.375′W	JF744856	JF744956	JF744787
SANG547	Gaspesie, Rte 132 E of Claridorme, Québec, Canada	Spribille & Wagner, 02.10.09, s.n.	49°07.689′N	64°44.277′W	JF744868	JF744957	JF744788
SANG550	Gaspesie, Québec, Canada	Spribille & Wagner, 01.10.09, s.n.	48°56.591′N	66°01.705′W	JF744870	JF744908	–
SANG551	Mt. Mansfield, Lamoille Co., Vermont, U.S.A.	Spribille & Wagner, 24.09.09, s.n.	44° 32.173′N	72° 48.897′W	JF744867	JF744958	JF744789
SANG559	Mt. Ascutney, Vermont, U.S.A.	Spribille 32193	43°26.744′N	72°27.104′W	JF744873	JF744959	JF744790
SANG591	Šumava Mtns., S. Bohemia, Czech Republic	Palice & Printzen s.n.	48°47.4′N	013°52.4′E	JF744876	JF744960	JF744791
SANG598	7.5 km E of Ladva village, Leningrad Oblast', Russia	Stepanchikova & Himelbrant s.n.	60°23′22‘‘N	35°11°27‘‘E	JF744869	JF744961	JF744792
SANG605	LaBiche River, Yukon Territory, Canada	Spribille 28305	60°09.037′N	124°05.385′W	JF744877	JF744987	–
SANG637	Loch an Eilein, Scotland, U.K.	Ellis s.n.	57°8′43.926‘‘N	3°50′15.319‘‘W	JF744871	–	JF744793
SANG775	Sokhondinskiy Zapovednik, Zabaikalskiy Krai, Russia	Yakovchenko s.n.	50° 52.429′N	113° 22.341′E	–	JF744962	–
Tephromela atra s.ampl.							
TEPH629	Fraser Canyon, British Columbia, Canada	Björk 18057	49°38.5′N	121°24.6′W	JF744875	JF744986	JF744821

Author's personal copy

Table 2
Markers and primers used in this study.

Locus	Abbreviation	Primer name	Primer sequence (5′–3′)	Source
Elongation factor 1-α	EF1-α	EF983	GCYCCYGGHCAYCGTGAYTTYAT	Rehner and Buckley (2005)
		EF2218R	ATGACACCRACRGCRACRGTYTG	Rehner and Buckley (2005)
Internal transcribed spacer	ITS	ITS1F	CTTGGTCATTTAGAGGAAGTAA	White et al. (1990)
		ITS4	TCCTCCGCTTATTGATATGC	White et al. (1990)
Mini-chromosome maintenance complex 7	MCM7	MCM7–709f	ACIMGIGTITCVGAYGTHAARCC	Schmitt et al. (2009)
		MCM71348rev	GAYTTDGCIACICCIGGRTCWCCCAT	Schmitt et al. (2009)

submitted to GenBank and are retrievable under the accession numbers given in Table 1.

2.2. Phylogenetic analyses

Alignments were performed using ClustalW (Thompson et al., 1994) and subsequently optimized by hand in BioEdit (Hall, 1999). Ambiguous and non-conserved regions were removed using Gblocks (Talavera and Castresana, 2007). Nucleotide substitution models were determined for each fragment and individually for the first, second and third codon position of protein-coding genes using jModelTest (Posada, 2008) according to the Akaike Information Criterion (AIC). Individual gene alignments were analyzed using a maximum likelihood (ML) and Bayesian Markov Chain Monte Carlo (MCMC) approach. The three fragments were tested for conflict in the phylogenetic signal using a partition homogeneity test implemented in PAUP* 4.0b10 (Swofford, 2002) using 500 bootstrap replicates and employing an heuristic search with simple addition of sequences. Maximum likelihood analyses were performed using the program PhyML (Guindon and Gascuel, 2003). Bootstrapping was carried out on 500 tree replicates. Bayesian MCMC analyses were performed using the program MrBayes v. 3.1.2 (Huelsenbeck and Ronquist, 2001). The analyses were performed using substitution models approximated by jModeltest (see above). For each analysis, a run with 8 million generations starting with a random tree and running six simultaneous heated chains was employed. Every 100th tree was sampled and saved to a file. The first 500,000 generations (5000 trees) were discarded as chain 'burn-in'. The program TRACER v. 1.5 (http://tree.bio.ed.ac.uk/software/tracer/) was used to assess whether likelihood values had reached stationarity within the allocated burn-in window by plotting log likelihood ratios against the number of generations. In addition, we examined the distributions of split frequencies using the online program AWTY (Nylander et al., 2007) to test whether runs had converged, independent of apparent stationarity detected in TRACER. Of the remaining 75,001 trees a majority consensus tree with averaged branch lengths and annotated with posterior probability values at every node was calculated using the sumt command in MrBayes. Only clades that received bootstrap values $\geq$70% in ML and posterior probabilities $\geq$0.95 were considered significant. Phylogenetic trees were visualized in TreeView (Page, 1996). Variable sites and nucleotide composition were calculated using MEGA 5 (Tamura et al., 2007); saturation plots were generated using DAMBE (Xia and Xie, 2001).

2.3. Polymorphism and divergence

In order to better visualize differences within and between clades, we employed three measures. Within clades, nucleotide diversity was quantified using the average number of nucleotide differences among sequences in a sample, π (Nei and Li, 1979). Divergence between clades was quantified using the pairwise average number of nucleotide substitutions per site between groups (D_{xy}, Nei and Kumar, 2000). Finally, genetic differentiation (*Fst*; Hudson et al., 1992) was calculated between clades as a complementary measure of distance weighted by haplotype frequencies within each clade. We defined the groups we compared based on clade assignment of each individual in the three gene phylogeny. Calculations of π and D_{xy} were carried out using DnaSP (Librado and Rozas, 2009) and *Fst* was calculated using Arlequin v. 3.11 (Excoffier et al., 2005).

2.4. Morphological and chemical analyses

To test whether our phylogenetic results could be matched by morphological traits, we sorted specimens under a Leica Wild M3Z dissecting scope and examined anatomical sections in water with a Zeiss Axioskop light microscope fitted with a ZeissAxioCam MRc5 digital camera; images of growth habit were digitally optimized using CombineZM open source image processing software (www.hadleyweb.pwp.blueyonder.co.uk/CZM/). Pigments were examined under the light microscope and named according to Meyer and Printzen (2000). In addition, we examined specimens for chemical patterns that could support phylogenetic differentiation using thin layer chromatography. This analysis was carried out on all specimens for which DNA sequences had also been obtained, using methods outlined by Culberson (1972) with modifications following Culberson and Johnson (1982). We used silica-coated glass plates (Macherey–Nagel 821 030) run their full length in solvent systems A, B′ and C. Aliphatic acids were visualized by immersing completely dried plates post-development into a tank of water for 1–2 s, quickly dripping off the plates and marking spots over the next 4–5 min.

3. Results

3.1. Data characteristics and model selection

We obtained a total of 247 new sequences, including 83 from EF1-α, 83 from ITS and 81 from Mcm7, including the first modern documentation of the species *M. glabrescens*. Following exclusion of positions with missing data, the sequences consisted of 697, 494 and 493 characters, respectively, for a combined total of 1684 characters (Table 3). The partition homogeneity test indicated no significant conflict between the three loci ($P = 0.69400$).

The nucleotide substitution models selected for our loci vary among genes and codon positions (Table 3). Bayesian phylogenetic analysis of gene trees was conducted using codon-based partitioning while models calculated for entire fragments were used in the partitioned concatenated analysis and for maximum likelihood calculations. Codon-based partitioning resulted in almost no difference in topology compared to calculations run with a single model applied to the whole fragment (data not shown). Stationarity was reached early in all gene trees (before 100,000 generations) and in the partitioned Bayesian analysis of concatenated data based on plotting of log likelihoods against generation. Comparisons of split frequencies between runs and in cumulative split frequency plots in AWTY likewise indicated that run convergence

Author's personal copy

Table 3
Sequence attributes of markers used in this study; *n* = number of sequences, var sites = variable sites (total in alignment/total minus outgroup and FUC600); selected model using jModeltest.

Data set/partition	Sites	*n*	Var sites	Average nucleotide composition				Selected model
				T(U)	C	A	G	
EF1-α (full dataset)	697	83	181/139	22.1	28.8	24.1	25.0	TPM1ef + G
Codon position 1	233		24/21	13	19.7	31.2	35.8	TIM3 + G
Codon position 2	232		17/15	25	23.6	33.7	17.4	TPM2uf + G
Codon position 3	232		140/103	28	43.2	7.4	21.6	TPM2uf + G
ITS	494	83	166/137	24.2	28.4	21.2	26.2	TrNef + G
MCM7 (full dataset)	493	81	183/136	24.4	26.2	29.0	20.4	HKY + G
Codon position 1	165		26/21	19	26.1	27.3	27.8	TrNef
Codon position 2	164		16/12	28	24.5	34.2	13.4	TIM3
Codon position 3	164		141/103	27	28.0	25.6	19.8	TPM2

had been reached well before the burn-in threshold of 500,000 generations.

Variability in the markers increased in the order of EF1-α (25.9% of sites variable) to ITS (33.6%) to Mcm7 (37.1%; Table 3). A considerable amount of this variability was derived from the outgroup and the single sequence of *M. fucatus* (FUC600) (Table 3). In the two protein-coding genes, the majority of variability was concentrated in the third codon position, in both cases with 77% of variable sites found at this position. Saturation plots (Supplementary Fig. S1) indicate continuous near-linear divergence of transitions and transversions over genetic distance in the case of EF1-α both with and without consideration of the outgroup, while in Mcm7 a transition plateau is reached at a Felsenstein 84 distance of about 1.4, suggesting that saturation has been reached at that position in Mcm7 (Supplementary Fig. S1C). This effect is however mitigated if the outgroup and sequence FUC600 are removed (Supplementary Fig. S1D).

3.2. Phylogenetic analysis of gene trees and geographic patterns

Maximum likelihood and Bayesian gene tree calculations produced concordant topologies for the concatenated data set (Fig. 1) and EF1-α (Supplementary Fig. S2), but topological differences were observed between the two methods at one node each in ITS and Mcm7 (Supplementary Figs. S3-S6). All gene trees and the partitioned analyses of the concatenated data provide strong support for *Mycoblastus affinis*, *M. glabrescens* and *M. sanguinarius* s.lat. as monophyletic groups (posterior probability = 1.0, bootstrap = 98–100%). Individuals of *M. alpinus* are nested within *M. affinis* in all loci and are not supported. *M. fucatus*, for which only ITS and Mcm7 was available, occurs outside of the group of studied species and consistently close to the outgroup, *Tephromela atra*. *M. japonicus*, for which only ITS was available, is strongly supported in this locus as sister to *M. affinis* (Fig. 1 and Supplementary Figs. S3 and S4). The sister group relationships of the species-level taxa are not well supported except for two cases: (1) *M. glabrescens* is supported as sister to *M. sanguinarius* s.lat. in both the Bayesian MCMC and ML Mcm7 phylogenies, as well as in the partitioned analyses of the concatenated data set; and (2) *M. affinis* is supported as sister to the group including *M. glabrescens* and *M. sanguinarius* s.lat. in the ML ITS phylogeny and both Mcm7 phylogenies as well as in the concatenated data set (Fig. 1).

Within *M. sanguinarius* s.lat., a deep and well supported split is found in the concatenated data set (Fig. 1) between a likewise well supported clade including specimens of the Tasmanian *M. sanguinarioides* (Clade I) and material of *M. sanguinarius* s.str. (Clade II). This relationship is also found in all gene phylogenies except the Mcm7 ML tree (Supplementary Fig. S6). Each of the two *M. sanguinarius* s.lat. clades is again split into recurrent groups. Within-clade patterns in Clade I (=*M. sanguinarioides*) differ between the three genes. In the topology of EF1-α and the concatenated analyses, the larger of two subclades shares the eastern North American-eastern Asian distribution of *M. sanguinarius* Clade IIb, while the smaller clade is restricted to western North America. The two geographical types are mixed in the ITS gene tree and in Mcm7 the Tasmanian clade is not supported. We recognize here two clades (Ia and Ib) in the concatenated data set corresponding to material from the southern and northern hemispheres, respectively.

Most of the six groups in Clade II (=*M. sanguinarius* s.str.) are strongly differentiated and recurrent between genes. 'Clade' IIa is in fact a terminal branch represented by a single specimen from the Yukon, Canada whose position within *M. sanguinarius* s.str. is unresolved; its chemistry and ecology also proved aberrant (see below). Clade IIb occurs primarily in eastern North America, the Russian Far East, and northern Sweden, with a single specimen from Alaska; it recurs in all three loci and is strongly supported in EF1-α, the Mcm7 ML analysis and in the concatenated data set. Clade IIb occupies a rather isolated position among the *M. sanguinarius* s.str. clades, occurring as sister to the rest of *M. sanguinarius* s.str. in the concatenated phylogeny (Fig. 1) and even together with Clade I in a strongly supported sister group to the rest of Clade II in the Mcm7 ML tree (Supplementary Fig. S6). Clade IIc is represented by a small number of individuals from Hokkaido, Japan and the Russian Far East. Clades IId, IIe and IIf are closely related and occur in all three loci, except in EF1-α where Clades IId and IIf are indistinguishable. Clade IId is found almost entirely in western North America, with a few specimens from northern Sweden; Clade IIe was found only in western North America; and Clade IIf was found only in Europe. All groups within *M. sanguinarius* s.str. are strongly supported in the partitioned Bayesian analysis of the concatenated data set, while only groups IIc, IId and IIe receive strong bootstrap support in the ML analysis.

3.3. Polymorphism and divergence

Pairwise divergence between clades measured in terms of average number of nucleotide substitutions per site (D_{xy}) was consistently highest, as would be expected, between the subclades of the major Clades I (=*M. sanguinarioides*) and II (=*M. sanguinarius*; Table 4). In the pairwise comparison of Clades I and II, ITS showed the greatest divergence, with values of 0.06240–0.07375 in ITS, followed by EF1-α (0.04790–0.05657) and Mcm7 (0.01623–0.04199). Lower D_{xy} values were observed between the subclades of Clade II, with the highest divergence here being found within Mcm7 (up to 0.02480), with similar D_{xy} values between ITS and EF1-α. The anomalous position of Clade IIb within the *M. sanguinarius* s.str. clade is again visible in the D_{xy} values, with Clade IIb exhibiting very low D_{xy} values in pairwise comparisons with Clade I (=*M. sanguinarioides*) and comparatively high D_{xy} values in pairwise matchups with Clades IIc–IIf.

Fst values were highest between clades in EF1-α (both within and between the subclades of Clades I and II), with intermediate

Author's personal copy

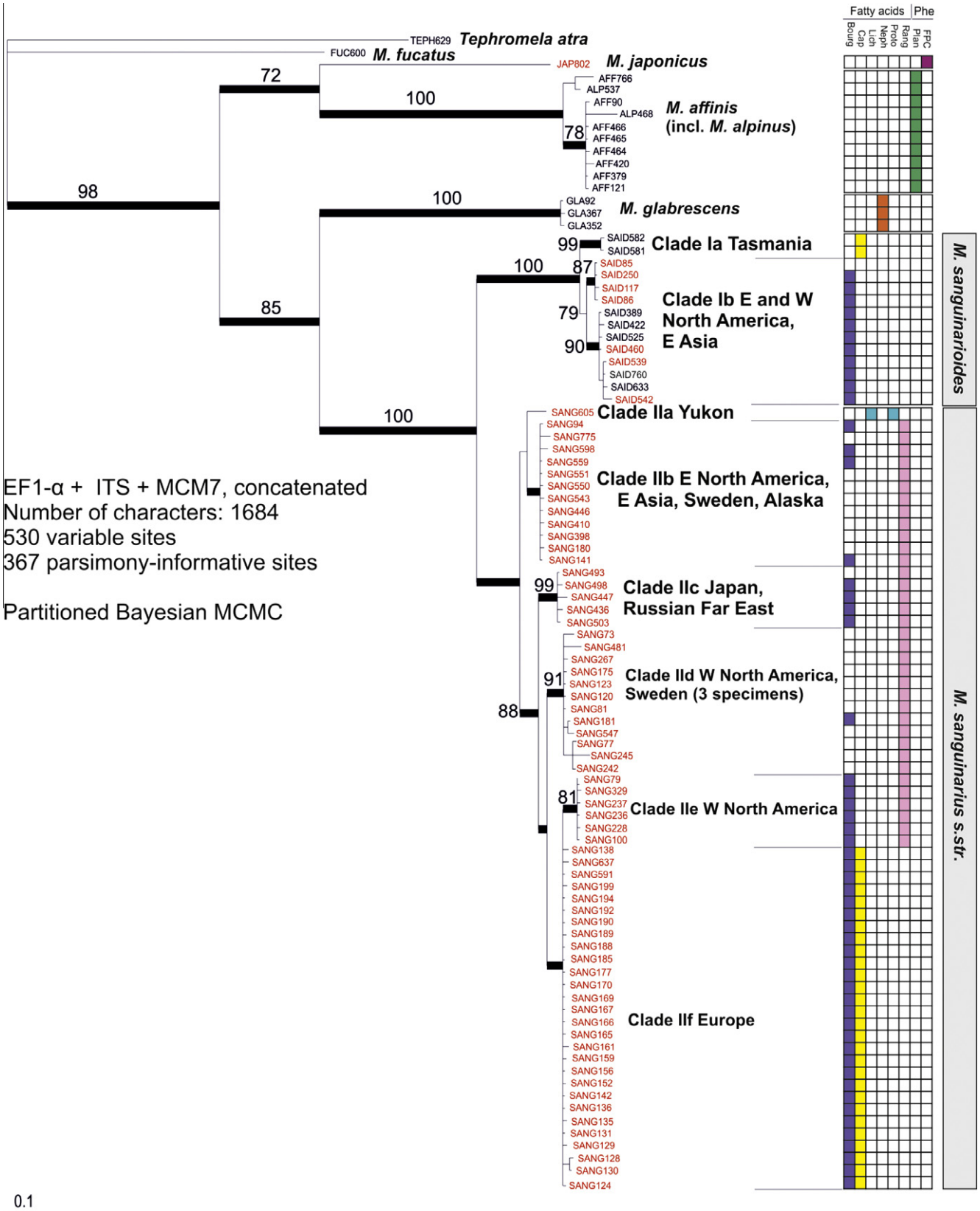

Fig. 1. Bayesian MCMC consensus tree of concatenated EF1-α, ITS and Mcm7 gene sequences. Posterior probabilities >95% are shown as thick branches; bootstrap support results of maximum likelihood analysis are shown where >70%. Names in red indicate individuals with the red pigment mysaquinone in the apothecia. Thallus secondary chemistry is shown in the bar to the right of the tree. Abbreviations: bourg, bourgeanic acid; cap, caperatic acid; lich, lichesterinic acid; neph, nephrosterinic acid; proto, protolichesterinic acid; rang, rangiformic acid; plan, planaic acid; FPC, fumarprotocetraric acid. Phe denotes phenolic compounds. All individuals also contain the depside atranorin.

Author's personal copy

Table 4
Genetic differentiation (*Fst* values, above diagonal), genetic divergence (D_{xy}, below diagonal) and within-clade nucleotide diversity (per site π, diagonal, in bold) in the subclades of the *Mycoblastus sanguinarius* group. π is zero when only one haplotype is present in a subclade. Clade IIa is not represented because it consists of only a single individual. *Fst* values: *pairwise comparison significant following Bonferroni correction ($P \leq 0.0012$).

	Ia	Ib	IIb	IIc	IId	IIe	IIf
EF1-α							
Clade Ia	**0.0000**	0.70370	1.00000	1.00000	0.98870	1.00000	0.99768
Clade Ib	0.00914	**0.0027**	0.97504*	0.94799*	0.96788*	0.96498*	0.98394*
Clade IIb	0.05208	0.05170	**0.0003**	1.00000*	0.96491*	1.00000*	0.98941*
Clade IIc	0.05031	0.04790	0.00661	**0.0000**	0.92221	1.00000	0.98240*
Clade IId	0.05267	0.05014	0.00855	0.00732	**0.0005**	0.80254*	0.04932
Clade IIe	0.05305	0.04966	0.00970	0.00859	0.00188	**0.0000**	0.94089*
Clade IIf	0.05657	0.05167	0.00952	0.00760	0.00041	0.00189	**0.0001**
ITS							
Clade Ia	**0.0087**	0.67706	0.98950	1.00000	0.98094*	0.99141	1.00000*
Clade Ib	0.01561	**0.0022**	0.94983*	0.94024*	0.94941*	0.93722*	0.97979*
Clade IIb	0.06240	0.06603	**0.0040**	0.97540*	0.94347*	0.94595*	0.99123*
Clade IIc	0.07069	0.06772	0.02107	**0.0000**	0.94967*	0.98039*	1.00000*
Clade IId	0.07375	0.06942	0.02010	0.01787	**0.0012**	0.88998*	0.97741*
Clade IIe	0.06653	0.06660	0.01322	0.01708	0.01363	**0.0009**	0.99393*
Clade IIf	0.07002	0.07005	0.01116	0.01325	0.01377	0.00907	**0.0000**
MCm7							
Clade Ia	**0.0000**	0.29622	1.00000	0.86813	0.89616	1.00000*	0.97961
Clade Ib	0.00517	**0.0056**	0.89676*	0.86768*	0.88373*	0.92231*	0.95262*
Clade IIb	0.01623	0.02268	**0.0000**	0.92225*	0.89605*	1.00000*	0.97221*
Clade IIc	0.03392	0.03986	0.02065	**0.0068**	0.51065*	0.84576*	0.89364*
Clade IId	0.03537	0.04013	0.02428	0.00837	**0.0031**	0.85075*	0.89819*
Clade IIe	0.03486	0.04036	0.02179	0.01270	0.01900	**0.0000**	0.79000*
Clade IIf	0.03628	0.04199	0.02062	0.00996	0.01781	0.00280	**0.0040**

values in ITS, and the lowest values in Mcm7 (Table 4). Two exceptions to the high values are the pairings of Clades IId and IIf, which are not distinguishable in EF1-α (see above and Supplementary Fig. S2) and accordingly have a low *Fst* value; and Clades IIc and IId in Mcm7, which both occur on a single well supported branch, with each Clade IIc sequence constituting a unique haplotype, lowering the *Fst* value. The sequence diversity within Clades IIc and IId is also expressed in terms of per site π values, which in Clade IIc is the highest of any clade (Table 4). Values for π were otherwise low overall, being the highest in clades with heterogeneous sequence assemblages, especially Clade Ib.

3.4. Morphological and chemical data

An initial comparison of material from Clades I and II did not reveal any obvious morphological differences. Specimens from Clade I tended to have pruinose young apothecia (Fig. 2A) surrounded by whitish thalline material, and the apothecia were flatter when mature than the apothecia of specimens from Clade II (Fig. 2D), but this was not a consistent predictor of clade assignment. Mysaquinone pigmentation was consistently found in Clade II but occasionally absent from specimens in Clade I, but its presence or absence in an apothecium was variable even within individuals from a single site. We detected slight differences of the hymenial pigmentation, with apothecia from specimens of Clade II possessing more intense pigmentation of *Cinereorufa*-green than individuals of Clade I. No differences were noticed in ascospore size. Both clades have one ascospore per ascus. However, systematic examination of apothecial cross-sections revealed that, without exception, all individuals of Clade I possessed microscopic birefringent crystals in the apothecial hymenium (Figs. 2C) which were always lacking in individuals of Clade II (Fig. 2F). The internal hymenial crystals are sometimes also externally visible in the form of a light pruina on the surface of the apothecia (Fig. 2A), especially when young, in contrast to the smooth, waxy black apothecia of *M. sanguinarius* (Fig. 2D).

Chemical profiles were obtained from all 82 specimens of *Mycoblastus sanguinarius* s.lat. and are depicted in Fig. 1. We found six distinct fatty acid combinations: bourgeanic acid alone (Bourg), caperatic acid alone (Cap), lichesterinic and protolichesterinic acid (Lich + Proto), rangiformic/norrangiformic acids alone (Rang), and the unique combinations Bourg + Rang and Bourg + Cap. One specimen (SAID85) had no detectable fatty acids after two runs. In addition, the fatty acid nephrosterinic acid (Neph) was detected in *M. glabrescens* and the depside planaic acid (Plan) and depsidone fumarprotocetraric acid (FPC) in *M. affinis* and *M. japonicus*, respectively. When tested categorically, fatty acid profiles in the *M. sanguinarius* complex are sufficiently correlated with clades ($X^2 = 370.8763$, df = 42, $p = <2.2 \times 10^{-16}$; φ-coefficient = 2.126707) that they can be used in part to predict clade assignment. The Bourg and Cap profiles are unique to clades Ia and Ib, respectively, and the Bourg + Cap profile is found only in Clade IIf. Clades IIb through IIe are united by a common motif of profiles with Rang alone or in combination with Bourg; both sets occur in western North America, where they always belong to either Clade IId (Rang alone; individual SANG181 is from Sweden) or Clade IIe (Bourg + Rang). A similar, though less pronounced pattern is evident between Clades IIb and IIc in eastern Asia (Fig. 1). We note that one of the characters heretofore used to distinguish *M. sanguinarioides* (Clade I) from *M. sanguinarius* (Clade II), namely that *M. sanguinarioides* has Cap and never Bourg, is not supported by our data, but that the two fatty acid profiles of *M. sanguinarioides* (Cap and Bourg) are so far unique to that clade as these substances always occur in combination with other substances in *M. sanguinarius* s.str. according to our data.

4. Discussion

4.1. Reassessing the circumscription of Mycoblastus sanguinarius

Our results suggest that considerable diversity is concealed behind what has been long regarded as a single, circumboreal lichen species. Specifically, our data support scenario number three in our introduction, namely that forms with the red pigment mysaquinone are distinct from the unpigmented *M. affinis*, and that there is more than one species involved. The first of these, *M. japonicus*,

Author's personal copy

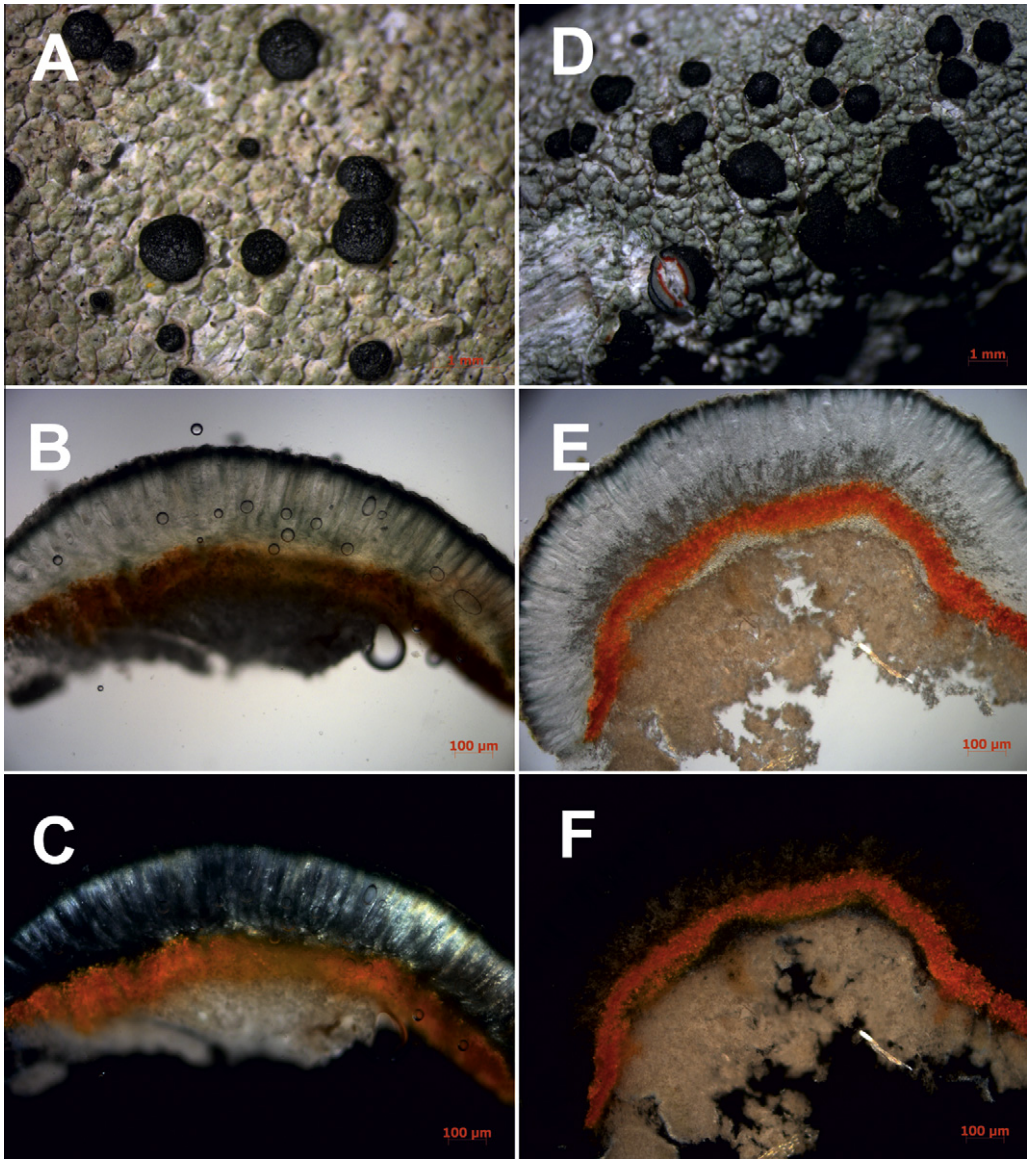

Fig. 2. Habit and key morphological characteristics of *Mycoblastus sanguinarioides* (A–C) and *M. sanguinarius* (D–F). A and D, habit; B and E, sections of apothecium, in water (light microscope); C and F, the same sections as in B and E shown in polarized light. A from Bijoux Falls, British Columbia (*Spribille 26158*, GZU), B–C from Chilkoot Trail, southeast Alaska (*Spribille 27038-C*, GZU) and D–F from Mt. Ascutney, Vermont (*Spribille 32196*, GZU).

is represented in our study by a single specimen, but has been previously recognized and will not be discussed further here. The second (=Clade I) corresponds to the recently described Tasmanian species *M. sanguinarioides* and is herewith reported as new to the northern hemisphere, where it is widespread and in fact more common than in the southern hemisphere. *M. sanguinarioides* is a classic example of a cryptic species, with specimens having passed through the hands of lichenologists since the middle of the 19th century and yet only once recognized as unique, by Nylander (1890), as *Lecidea sanguinaria* var. *lecanoroidea*, from Japan (holotype specimen at Helsinki, seen by the first author). It was not recognized at the species level until Kantvilas (2009) provided it a name based on material from Tasmania, where it occurs disjunctly. Kantvilas' circumscription of *M. sanguinarioides* almost completely overlaps with characters also found in *M. sanguinarius*, and the morphological characters detected in the present study (presence of hymenial crystals) are much more reliable for distinguishing it from *M. sanguinarius*. Mysaquinone is a facultative pigment in the Tasmanian populations (Kantvilas, 2009) and the same holds true in populations we sampled in the Russian Far East, where it almost always lacks the pigment, and northeastern North America, where pigment-deficient forms are common. Unpigmented forms of *M. sanguinarioides* likely account for many reports of *M. affinis* from these regions. Nearly all specimens sampled in western North America contained this pigment.

The third red-pigmented species (Clade II) corresponds to *M. sanguinarius* s.str. Clade II is an interesting case because it is a well supported monophyletic group only in the gene tree of EF1-α and the concatenated three-gene data set; in the analyses of ITS and Mcm7 it is not supported. One reason for this may be the relatively isolated position of its 'eastern' clades, especially Clade IIb. Clades IIa through IIc occupy an isolated position from the rest of *M. sanguinarius* in the ITS phylogeny and are even reciprocally monophyletic to it in EF1-α. Individuals of Clade IIb are however morphologically and chemically closer to *M. sanguinarius* s.str.; they lack the birefringent hymenial crystals typical of *M. sanguinarioides* and share the same chemical profile as *M. sanguinarius* Clade IId. Resolving the relationships and distinctness of this clade may be connected to the status of the chemically unique individual SANG605 (Clade IIa), which is close to Clade IIb, and which is

Author's personal copy

known so far from a single mountain in the Yukon, Canada, where it was found growing over rock. It cannot be ruled out that potentially undiscovered strains close to Clade IIb might remain to be discovered and could help resolve its relationships.

The placement of *Mycoblastus alpinus* nested within *M. affinis* appears to lend support to recent suspicions of northern European taxonomists that the two may be conspecific (Tønsberg, 1992; James and Watson, 2009). However, variation within *M. affinis* deserves further sampling as at least two individuals are significantly differentiated from the core of *M. affinis* especially in the EF1-α phylogram. At the same time, the strong support for the distinctness of *M. glabrescens* is noteworthy as currently the only way to distinguish it from *M. affinis*, other than DNA, is by chemistry. *M. glabrescens* was a forgotten species for more than a century until it was resurrected by Kantvilas (2009), and the first modern collections are those reported in this study.

The mycobiont of *M. sanguinarius* s.lat. joins a suite of other fungi in which molecular-level studies have revealed unforeseen geographic structure and cryptic lineages in what were previously thought large continuous ranges. *Amanita muscaria*, a circumboreal ectomycorrhizal fungus occurring in many of the same general areas as *M. sanguinarius*, has also been shown to possess strong geographic differentiation within its global population (Geml et al., 2006, 2008), although the geographic patterns do not closely approximate those we have found. Molecular investigations have revealed cryptic fungal species lineages in widespread and well-known lichen species such as *Letharia vulpina* (Kroken and Taylor, 2001) and *Parmelina quercina* (Argüello et al., 2007; for a review see Crespo and Pérez-Ortega, 2009). To the extent this can be considered a trend in other groups, it signals that lichens are conservative in adhering to or reverting to morphological motifs, rendering recognition of phylogenetic species challenging.

4.2. Phylogenetic signal among the markers

Much of the phylogenetic signal in our study is contributed by ITS and Mcm7, with the least variability in EF1-α. In general, alignment of all three fragments was straightforward except for several short variable regions in ITS and a variable 50 BP section around position 500 (in our alignment) in EF1-α, which were excised by Gblocks. Of particular interest was the performance of the Mcm7 gene. Mcm7 has only recently begun to be used for phylogenetic studies in lichenized fungi (Schmitt et al., 2009; Leavitt et al., 2011). Mcm7 is a single-copy gene coding for one of a family of DNA replication licensing factors, originally identified from yeast, and later from higher eukaryotes (Kearsey and Labib, 1998). Despite the highly degenerated primers, we found it relatively easy to obtain from fresh DNA extractions although the ability to obtain sequencable PCR products quickly declined over time, unlike with multicopy ribosomal DNA regions such as ITS. The phylogenetic signal provided by Mcm7, as shown in Supplementary Figs. S5 and S6, is more sub-structured than that of EF1-α and comparable to that of ITS. Mcm7 exhibited the lowest level of sequence divergence between *M. sanguinarioides* and *M. sanguinarius* in pairwise nucleotide diversity and the lowest *Fst* values compared to EF1-α and ITS. Of the three markers used here, Mcm7 reported the highest proportion of variable sites and a higher level of ts-saturation at the third codon position than EF1-α (Supplementary Fig. S1). The detection of any kind of saturation at such a low taxonomic level contrasts with the statement by Schmitt et al. (2009) that Mcm7 distinguishes itself from ribosomal markers such as ITS and mitochondrial small subunit in not exhibiting saturation, making it suitable for use at the genus level and above. The level of saturation and variability is clearly reduced when excluding the most dissimilar sequences in our dataset (*Mycoblastus fucatus* and the outgroup; Supplementary Fig. S1), but the observed ts-saturation with inclusion of even closely related taxa such as these suggests that saturation and homoplasy should be carefully monitored when using this marker to recover gene phylogenies.

4.3. Evolutionary significance of chemotypes

Mycoblastus sanguinarius is not unique amongst lichens in including an array of fatty acid profiles. Indeed, many common lichen genera include species with multiple fatty acid strains. While these strains have sometimes been accorded taxonomic rank (e.g., *Cladonia*: Culberson, 1986; *Lepraria*: Fehrer et al., 2008), they are more often treated as 'chemotypes' (e.g., *Parmelia*: Hale, 1987; *Tephromela* s.lat.: Haugan and Timdal, 1994). Fatty acids were poorly studied in early studies of lichen secondary chemistry and it was long believed they were not of taxonomic significance. Though richly represented in some of the largest lichen genera (*Lecanora*, *Pertusaria*) they have been all but omitted from reviews of lichen chemistry (Hawksworth, 1976; Lumbsch, 1998). Their functional significance is not well understood, but available evidence points to a role in chemical protection. Protolichesterinic acid, a fatty acid reported here from *Mycoblastus* for the first time, has been shown to have antibiotic properties (Huneck, 2001); it is the active compound of 'Icelandic moss' used in pharmaceuticals (Ingolfsdottir et al., 1997) and has been shown to inhibit bacterial growth in culture (Türk et al., 2003). Lawrey (1983) found evidence of caperatic acid, which we found in both *M. sanguinarioides* and *M. sanguinarius*, being an active antiherbivory agent in the lichen genus *Allocetraria*.

A noteworthy feature of fatty acid variation in *M. sanguinarius* s.lat. is the recurring nature of fatty acid profiles. Chemotype development in *M. sanguinarioides* and *M. sanguinarius* appears to have bifurcated in parallel, with both taxa developing similar Cap- and Bourg-dominated profiles. Parallelism also occurs within *M. sanguinarius* s.str. with two of the fatty acid profiles we found (Bourg + Rang and Rang), occurring side-by-side in two regions (western North America and East Asia), though belonging to different clades in each case. In some cases we found different clades/chemotypes to occur side-by-side in the same forest stand (unpublished data). Various instances of chemical parallelism in lichens have been reported, including several involving fatty acids. Clayden (1992) reported two geographically separated fatty acid strains developing parallel phenolic chemotypes in *Arctoparmelia*. In an apparent extension of the phenomenon, Culberson and Culberson (1973) reported parallel morphotypes developing in parallel chemotypes in the genus *Parmotrema* and later (1977) in the genus *Cetrelia*; Leuckert and Poelt (1989) found parallelism of xanthone chemotypes in *Lecanora*. All of these cases of chemical parallelism have in common their occurrence at low taxonomic rank, i.e., they are presumably recent descendants of a common ancestor.

Hale (1961), in an early review of the value of lichen chemistry in systematics, presciently noted that "we cannot overlook the possibility that strain formation is a forerunner of morphological differentiation and a process of speciation". Our data provide further evidence that taxonomists and evolutionary biologists should be careful before dismissing chemotypes as within-taxon 'variability' as has sometimes been done in the past. Culberson et al. (1985) suspected a close connection between chemosyndromic development and evolution and explored the potential role of photobiont interaction in controlling this process. Our data strongly support the connection between genotype and chemotype in the fungus of *Mycoblastus sanguinarius*, which while not ruling out a role for the photobiont in fine-scale chemical differentiation during incipient speciation events, does confirm that genetic differentiation becomes fixed in the fungal partner. More data are required to triangulate on this phenomenon and narrow down the possible role of the photobiont in fatty acid profile expression.

Author's personal copy

Secondary substance profiles in lichens, including difficult-to-detect or 'accessory' substances, can provide a window into diversification processes across ecological and geographical space and may be the early external manifestations of as yet unclarified selective processes.

4.4. Conclusions

Estimates of the true number of species of fungi range as high as 1.5 million (Hawksworth, 1991), whereby only about 80,000 have been described until now, including nearly 19,000 lichenized and lichenicolous fungi (Feuerer and Hawksworth, 2007). 'Cryptic species' have been put forward as a candidate group to account for some of the substantial discrepancy between these numbers (Hawksworth, 2001; Crespo and Pérez-Ortega, 2009), and the tropics are frequently invoked as the regions to search for the overlooked taxa (Hawksworth and Rossman, 1997). There are indications however that, for lichenized fungi at least, some of the highest lichen species diversity has so far been found at high latitudes (Spribille et al., 2010). Circumboreal species complexes like that of *M. sanguinarius* and other common lichens may prove to be fruitful taxonomic groups for mining previously unsuspected biodiversity as the focus of on-the-ground research shifts from identification key-based floristics to molecular-assisted biodiversity inventory.

Acknowledgments

We would like to thank Frances Anderson, Peter Bilowitz, Curtis Björk, Stephen Clayden, Paweł Czarnota, Chris Ellis, Trevor Goward, Josef Hafellner, Celia Hampton-Miller, Dmitry Himelbrant, Håkon Holien, Lucia Muggia, Peter Nelson, Yoshihito Ohmura, Zdeněk Palice, Sergio Pérez-Ortega, Christian Printzen, Walter Obermayer, Irina Stepanchikova, Göran Thor, Tor Tønsberg, Viktoria Wagner, Mats Wedin, Ken Wright and Lidia Yakovchenko, who either collected fresh material for us or assisted with sampling. Gintaras Kantvilas is especially thanked for providing us with fresh material of *Mycoblastus sanguinarioides* from Tasmania. We also thank Bureinskiy Zapovednik, Russia, Reserva Integral de Muniellos, Spain, and Denali and Klondike Gold Rush National Parks, USA for permission to collect in these protected areas. M. Grube and V. Wagner helped improve the manuscript. This project was funded by the Austrian Science Foundation (FWF) under Grant Number P21052-B16 (Circumboreal Lichen Diversification Project).

Appendix A. Supplementary material

Supplementary data associated with this article can be found, in the online version, at doi:10.1016/j.ympev.2011.03.021.

References

Ahti, T., 1977. Lichens of the boreal coniferous zone. In: Seaward, M.R.D. (Ed.), Lichen Ecology. Academic Press, London, pp. 145–181.

Anders, J., 1928. Untersuchungen über *Mycoblastus sanguinarius* (L.) Norm., *M. alpinus* (Fr.) Kernst. und *M. melinus* (Krph.) Hellb. Hedwigia 68, 87–92.

Andreev, M.P., Dobrysh, A.A., Golubkova, N.S., Himelbrant, D.E., Kataeva, O.A., Kotlov, Y.V., Makarova, I.I., Titov, A.N., Tolpysheva, T.Y., Urbanavichene, I.N., Urbanavichus, G.P., 2008. Handbook of the lichens of Russia. 10. Nauka, St. Petersburg. 515 pp (in Russian).

Argüello, A., del Prado, R., Cubas, P., Crespo, A., 2007. *Parmelina quercina* (Parmeliaceae, Lecanorales) includes four phylogenetically supported morphospecies. Biol. J. Linnean Soc. 91, 455–467.

Brodo, I.M., Sharnoff, S.D., Sharnoff, S., 2001. Lichens of North America. Yale University Press, New Haven, 795 pp.

Buschbom, J., Mueller, G.M., 2006. Testing "species-pair" hypotheses: evolutionary processes in the lichen-forming species complex *Porpidia flavocoerulescens* and *Porpidia melinodes*. Mol. Biol. Evol. 23, 574–586.

Clayden, S.R., 1992. Chemical divergence of eastern North American and European populations of *Arctoparmelia centrifuga* and their sympatric usnic acid-deficient chemotypes. Bryologist 95, 1–4.

Crespo, A., Pérez-Ortega, S., 2009. Cryptic species and species pairs in lichens: a discussion on the relationship between molecular phylogenies and morphological characters. Anales del Jardín Botánico de Madrid 66S1, 71–81.

Crespo, A., Molina, M.C., Blanco, O., Schroeter, B., Sancho, L.G., Hawksworth, D.L., 2002. RDNA ITS and β-tubulin gene sequence analyses reveal two monophyletic groups within the cosmopolitan lichen *Parmelia saxatilis*. Mycological Research 106, 788–795.

Culberson, C.F., 1972. Improved conditions and new data for the identification of lichen products by a standardized thin-layer chromatographic method. J. Chromatogr. 72, 113–125.

Culberson, C.F., 1986. Biogenetic relationships of the lichen substances in the framework of systematics. Bryologist 89, 91–98.

Culberson, W.L., Culberson, C.F., 1973. Parallel evolution in the lichen-forming fungi. Science 180, 196–198.

Culberson, W.L., Culberson, C.F., 1977. Chemosyndromic variation in lichens. Syst. Bot. 1, 325–339.

Culberson, C.F., Johnson, A., 1982. Substitution of methyl tert.-butyl ether for diethyl ether in Standardized thin-layer chromatographic method for lichen products. J. Chromatogr. 238, 438–487.

Culberson, C.F., Culberson, W.L., Johnson, A., 1985. Does the symbiont alga determine chemotype in lichens? Mycologia 77, 657–660.

Divakar, P.K., Figueras, G., Hladun, N., Crespo, A., 2010. Molecular phylogenetic studies reveal an undescribed species within the North American concept of *Melanelixia glabra* (Parmeliaceae). Fungal Divers. 42, 47–55.

Excoffier, L., Laval, G., Schneider, S., 2005. Arlequin ver. 3.0: an integrated software package for population genetics data analysis. Evol. Bioinf. Online 1, 47–50.

Fehrer, J., Slavíkova-Bayerová, Š., Orange, A., 2008. Large genetic divergence of new, morphologically similar species of sterile lichens from Europe (*Lepraria*, Stereocaulaceae, Ascomycota): concordance of DNA sequence data with secondary metabolites. Cladistics 24, 443–458.

Feuerer, T., Hawksworth, D.L., 2007. Biodiversity of lichens, including a world-wide analysis of checklist data based on Takhtajan's floristic regions. Biodiversity and Conservation 16, 85–98.

Geml, J., Laursen, G.A., O'Neill, K., Nusbaum, H.C., Taylor, D.L., 2006. Beringian origins and cryptic speciation events in the fly agaric (*Amanita muscaria*). Mol. Ecol. 15, 225–239.

Geml, J., Tuloss, R.E., Laursen, G.A., Sazanova, N.A., Taylor, D.L., 2008. Evidence for strong inter- and intracontinental phylogeographic structure in *Amanita muscaria*, a wind-dispersed ectomycorrhizal basidiomycete. Mol. Phylogen. Evol. 48, 694–701.

Geml, J., Kauff, F., Brochmann, F., Taylor, D.L., 2010. Surviving climate changes: high genetic diversity and transoceanic gene flow in two arctic–alpine lichens, *Flavocetraria cucullata* and *F. Nivalis* (Parmeliaceae, Ascomycota). J. Biogeogr. 37, 1529–1542.

Guindon, S., Gascuel, O., 2003. A simple, fast and accurate algorithm to estimate large phylogenies by maximum likelihood. Syst. Biol. 52, 696–704.

Hale, M.E., 1961. Lichen Handbook. Smithsonian Institution, Washington, DC, 178 pp.

Hale, M.E., 1987. A monograph of the lichen genus *Parmelia* Acharius sensu stricto (Asocmycotina: Parmeliaceae). Smithsonian Contr. Bot. 66, 1–55.

Hall, T.A., 1999. BioEdit: a user-friendly biological sequence alignment editor and analysis program for Windows 95/98/NT. Nucleic Acids Symp. Ser. 41, 95–98.

Haugan, R., Timdal, E., 1994. *Tephromela perlata* and *T. talayana*, with notes on the *T. aglaea*-complex. Graphis Scripta 6, 17–26.

Hawksworth, D.L., 1976. Lichen chemotaxonomy. In: Brown, D.H., Hawksworth, D.L., Bailey, R.H. (Eds.), Lichenology: Progress and Problems. Academic Press, London, pp. 139–184.

Hawksworth, D.L., 1991. The fungal dimension of biodiversity: magnitude, significance, and conservation. Mycological Research 95, 641–655.

Hawksworth, D.L., 2001. The magnitude of fungal diversity: the 1.5 million species estimate revisited. Mycol. Res. 105, 1422–1432.

Hawksworth, D.L., Rossman, A.Y., 1997. Where are all the undescribed fungi? Phytopathology 87, 888–891.

Hudson, R.R., Slatkin, M., Maddison, W.P., 1992. Estimation of levels of gene flow from DNA sequence data. Genetics 132, 583–589.

Huelsenbeck, J.P., Ronquist, F., 2001. MRBAYES, Bayesian inference of phylogenetic trees. Bioinformatics 17, 754–755.

Huneck, S., 2001. New results on the chemistry of lichen substances. Prog. Chem. Organic Nat. Prod. 81, 1–313.

Huneck, S., Schmidt, J., 1995. Neue Flechtenanalysen aus verschiedenen Verwandtschaftskreisen. In: Daniëls, F.J.A., Schulz, M., Peine, J. (Eds.), Flechten Follmann. Contributions to lichenology in honour of Gerhard Follmann. Botanical Institute, University of Cologne, Cologne, pp. 27–41.

Ingolfsdottir, K., Hjalmarsdottir, M.A., Sigurdsson, A., Gudjonsdottir, G.A., Brynjolfsdottir, A., Steingrimsson, O., 1997. In vitro susceptibility of *Helicobacter pylori* to protolichesterinic acid from the lichen *Cetraria islandica*. Antimicrob. Agents Chemother. 41, 215–217.

James, P.W., Watson, M.F., 2009. Mycoblastus. In: Smith, C.W., Aptroot, A., Coppins, B.J., Fletcher, A., Gilbert, O.L., James, P.W., Wolseley, P.A. (Eds.), The Lichens of Great Britain and Ireland. British Lichen Society, Natural History Museum, London, pp. 615–618.

Kantvilas, G., 2009. The genus *Mycoblastus* in the cool temperate Southern Hemisphere, with special reference to Tasmania. Lichenologist 41, 151–178.

Author's personal copy

Kearsey, S.E., Labib, K., 1998. MCM proteins: evolution, properties, and role in DNA replication. Biochim. Biophys. Acta 1398, 113–136.
Kroken, S., Taylor, J.W., 2001. A gene genealogical approach to recognize phylogenetic species boundaries in the lichenized fungus *Letharia*. Mycologia 93, 38–53.
Lawrey, J.D., 1983. Vulpinic and pinastric acids as lichen antiherbivore compounds: contrary evidence. Bryologist 86, 365–369.
Leavitt, S.D., Johnson, L., St. Clair, L.L., 2011. Species delimitation and evolution in morphologically and chemically diverse communities of the lichen-forming genus *Xanthoparmelia* (Parmeliaceae, Ascomycota) in western North America. Am. J. Bot. 98, 1–14.
Leuckert, C., Poelt, J., 1989. Studien über die *Lecanora rupicola*-Gruppe in Europa (Lecanoraceae). Nova Hedwigia 49, 121–167.
Librado, P., Rozas, J., 2009. DnaSP v5: a software for comprehensive analysis of DNA polymorphism data. Bioinformatics 25, 1451–1452.
Linnaeus, C., 1753. Species plantarum, exhibentes plantas rite cognitas ad genera relatas, cum differentiis specificis, nominibus trivialibus, synonymis selectis, locis natalibus, secundum systema sexuale digestas. Holmiae, 1231 pp.
Lumbsch, H.T., 1998. The use of metabolic data in lichenology at the species and subspecific levels. Lichenologist 30, 357–367.
Meyer, B., Printzen, C., 2000. Proposal for a standardized nomenclature and characterization of insoluble lichen pigments. Lichenologist 32, 571–583.
Nei, M., Kumar, S., 2000. Molecular Evolution and Phylogenetics. Oxford University Press, USA, 333 p.
Nei, M., Li, W.H., 1979. Mathematical model for studying genetic variation in terms of restriction endonucleases. Proc. Natl. Acad. Sci. USA 76, 5269–5273.
Nylander, W., 1890. Lichenes japoniae. Accedunt observationibus lichenes insulae Labuan. P. Schmidt, Paris, 122 pp.
Nylander, J.A., Wilgenbusch, J.C., Warren, D.L., Swofford, D.L., 2007. AWTY (are we there yet?): a system for graphical exploration of MCMC convergence in Bayesian phylogenetics. Bioinformatics 24, 581–583.
Page, R.D.M., 1996. Treeview: an application to display phylogenetic trees on personal computers. Comput. Appl. Biosci. 12, 357–358.
Posada, D., 2008. JModelTest: phylogenetic model averaging. Mol. Biol. Evol. 25, 1253–1256.
Printzen, C., 2008. Uncharted terrain: the phylogeography of arctic and boreal lichens. Plant Ecol. Div. 1, 265–271.
Rehner, S.A., Buckley, E., 2005. A *Beauveria* phylogeny inferred from nuclear ITS and EF1-α sequences: evidence for cryptic diversification and links to *Cordyceps* teleomorphs. Mycologia 97, 84–98.
Schauer, T., 1964. Die Flechtengattung *Mycoblastus* in Mitteleuropa. Nova Hedwigia 8, 301–310.
Schmitt, I., Crespo, A., Divakar, P.K., Fankhauser, J., Herman-Sackett, E., Kalb, K., Nelson, M.P., Nelson, N.A., Rivas-Plata, E., Schimp, A.D., Widhelm, T., Lumbsch, H.T., 2009. New primers for promising single copy genes in fungal phylogenetics and systematics. Persoonia 23, 35–40.
Spribille, T., Pérez-Ortega, S., Tønsberg, T., Schirokauer, D., 2010. Lichens and lichenicolous fungi of the Klondike Gold Rush National Historic Park, Alaska, in a global biodiversity context. Bryologist 113, 439–515.
Swofford, D.L., 2002. PAUP*. Phylogenetic Analysis Using Parsimony. (*and Other Methods). Version 4. Sinauer Associates, Sunderland, Massachusetts.
Talavera, G., Castresana, J., 2007. Improvement of phylogenies after removing divergent and ambiguously aligned blocks from protein sequence alignments. Syst. Biol. 56, 564–577.
Tamura, K., Dudley, J., Nei, M., Kumar, S., 2007. *MEGA4*: molecular evolutionary genetics analysis (MEGA) software version 4.0.. Mol. Biol. Evol. 24, 1596–1599.
Thompson, J.D., Higgins, D.G., Gibson, T.J., 1994. Clustal W: improving the sensitivity of progressive multiple sequence alignment through sequence weighting, position-specific gap penalties and weight matrix choice. Nucl. Acids Res. 22, 4673–4680.
Tønsberg, T., 1992. The sorediate and isidiate, corticolous, crustose lichens in Norway. Sommerfeltia 14, 1–331.
Türk, A.Ö., Yılmaz, M., Kıvanç, M., Türk, H., 2003. The antimicrobial activity of extracts of the lichen *Cetraria aculeata* and its protolichesterinic acid constituent. Zeitschr. Naturforsch. 58c, 850–854.
Wainio, E., 1909. Lichenes in viciniis stationis hibernae expeditionis Vegae prope pagum Pitlekai in Sibiria septentrionali a Dre. E. Almquist collecti. Praefationem scripsit F. Almquist. Arkiv Botanik 8, 11–175.
White, T.J., Bruns, T., Lee, S., Taylor, J.W., 1990. Amplification and direct sequencing of fungal ribosomal RNA genes for phylogenetics. In: Innis, M.A., Gelfand, D.H., Sninsky, J.J., White, T.J. (Eds.), PCR Protocols: A Guide to Methods and Applications. Academic Press, Inc., New York, pp. 315–322.
Xia, X., Xie, Z., 2001. DAMBE: data analysis in molecular biology and evolution. J. Heredity 92, 371–373.